Crystal-field interaction at the thulium site in $TmBa_2Cu_4O_8$



1998 J. Phys.: Condens. Matter 10 8269

(http://iopscience.iop.org/0953-8984/10/37/013)

J. Phys.: Condens. Matter **10** (1998) 8269–8278. Printed in the UK PII: S0953-8984(98)93377-X

# Crystal-field interaction at the thulium site in $TmBa_2Cu_4O_8$

G A Stewart†, S J Harker† and D M Pooke‡

† School of Physics, University College, The University of New South Wales, Australian Defence Force Academy, Canberra ACT 2600, Australia

‡ The New Zealand Institute for Industrial Research, PO Box 31310, Lower Hutt, New Zealand

Received 8 April 1998, in final form 3 July 1998

**Abstract.** Mössbauer spectroscopy is used to monitor the $^{169}$Tm quadrupole interaction for the superconductor $TmBa_2Cu_4O_8$ as a function of temperature. Qualitative comparison with other $^{169}$Tm results supports earlier claims that the $Tm^{3+}$ rank-2 crystal-field contribution lies between that for $TmBa_2Cu_3O_7$ and that for $TmBa_2Cu_3O_6$. However, there is quantitative disagreement with crystal-field parameters determined elsewhere for $HoBa_2Cu_4O_8$.

## 1. Introduction

Considerable experimental effort has been directed at characterizing the crystal field (CF) for the rare-earth site of the 1–2–3-type ($RBa_2Cu_3O_{7-\delta}$, R = rare earth) high-temperature superconductors and in investigating how it is influenced by oxygen deficiency ($0 < \delta < 1$). This is because the CF at the rare-earth ions is sensitive not only to the structural arrangement of the oxygen nearest neighbours but also to their effective charges. The charges are dependent on the degree of charge transfer which is, in turn, linked with the existence of superconductivity in the Cu–O planes. More recently, crystal-field data for the related 1–2–4-type ($RBa_2Cu_4O_8$) superconductors have become available.

As long as higher electronic terms of a trivalent rare-earth ion can be ignored, the CF perturbation of the ground multiplet can be represented by a Hamiltonian of the form

$$\mathcal{H}_{\mathrm{CF}} = \sum_{n,m} B_n^m O_n^m(J) = \sum_{n,m} A_n^m \theta_n O_n^m(J) \tag{1}$$

where $J$ is the total angular momentum quantum number, $B_n^m$ are CF parameters and the $\theta_n$ are rare-earth-specific factors associated with the Stevens equivalent operators, $O_n^m(J)$. The $A_n^m$ are better suited to comparison of results for isostructural compounds of different rare earths. The actual number of CF terms required depends on the local site symmetry. For the orthorhombic $TmBa_2Cu_3O_{7-\delta}$ and $TmBa_2Cu_4O_8$ structures [1, 2], the rare-earth site symmetry is orthorhombic $D_{2h}$ ($mmm$) with a CF Hamiltonian which can be expressed in its simplest form as

$$\mathcal{H}_{\mathrm{CF}} = B_2^0 O_2^0 + B_2^2 O_2^2 + B_4^0 O_4^0 + B_4^2 O_4^2 + B_4^4 O_4^4 + B_6^0 O_6^0 + B_6^2 O_6^2 + B_6^4 O_6^4 + B_6^6 O_6^6. \tag{2}$$

With increasing oxygen depletion, the orthorhombic structure of $RBa_2Cu_3O_7$ transforms to the tetragonal structure of $RBa_2Cu_3O_6$ [3] with tetragonal $D_{4h}$ ($4/mmm$) rare-earth site symmetry and a CF Hamiltonian of the form

$$\mathcal{H}_{\mathrm{CF}} = B_2^0 O_2^0 + B_4^0 O_4^0 + B_4^4 O_4^4 + B_6^0 O_6^0 + B_6^4 O_6^4. \tag{3}$$

0953-8984/98/378269+10$19.50  

The 1–2–3 and 1–2–4 systems are members of a homologous series of compounds with the general formula $R_2Ba_4Cu_{6+n}O_{14+n}$, with $n = 0$ and $n = 2$ respectively. In this series the rare-earth layers are essentially unchanged. Furthermore, the process of oxygen depletion of the 1–2–3 compounds involves oxygen sites that are not directly associated with the rare-earth layer. From a local perspective, the rare-earth site is thus very similar for all three compounds with the rare-earth ion surrounded by eight oxygens in the form of a slightly distorted cube. For this reason, the $A_n^m$-parameters for the long-range rank-2 ($n = 2$) CF component are expected to vary most from compound to compound, while those for the short-range rank-4 ($n = 4$) and rank-6 ($n = 6$) CF components are expected to remain relatively constant. With increasing charge depletion of the 1–2–3 compounds, the parameters $A_2^2$, $A_4^2$, $A_6^2$ and $A_6^6$ are expected to decrease monotonically to zero as required by (3).

**Table 1.** A summary of crystal-field parameters, $A_n^m = B_n^m/\theta_n$ ($cm^{-1}$), reported elsewhere in the literature for the techniques of Mössbauer effect spectroscopy (ME), inelastic neutron scattering (INS), magnetic susceptibility ($\chi$) and nuclear magnetic resonance (NMR). Except for $^{155}$Gd Mössbauer spectroscopy, for which the electric field gradients (parenthesized) have been converted to crystal-field parameters for R = Tm, all of the parameters are for the R as indicated.

| Method | $A_2^0$ | $A_2^2$ | $A_4^0$ | $A_4^2$ | $A_4^4$ | $A_6^0$ | $A_6^2$ | $A_6^4$ | $A_6^6$ |
|---|---|---|---|---|---|---|---|---|---|
| $RBa_2Cu_3O_7$ (orthorhombic) | | | | | | | | | |
| Gd ME [10] | 128.8 | 70.8 | | | ($V_{zz} = -5.99 \times 10^{21}$ V m$^{-2}$, $\eta = 0.55$) | | | | |
| Gd ME [11] | 133.3 | 50.7 | | | ($V_{zz} = -6.2 \times 10^{21}$ V m$^{-2}$, $\eta = 0.38$) | | | | |
| Ho INS [12] | 167.0 | 72.6 | −220.4 | 14.5 | 1017.3 | 28.1 | −16.8 | 841.7 | −11.8 |
| Tm ME [13] | 120.4 | 46.1 | −187.6 | 12.4 | 866.0 | 23.9 | −14.3 | 716.5 | −10.1 |
| Ho INS [14] | 217.4 | 93.8 | −238.4 | −235.1 | 1098.2 | 29.5 | −161.8 | 915.6 | −14.0 |
| Ho INS [5] | 142.4 | 96.8 | −274.2 | 29.0 | 1301.0 | 32.0 | −20.2 | 939.6 | −3.2 |
| $RBa_2Cu_3O_{6.65}$ (orthorhombic) | | | | | | | | | |
| Ho INS [5] | 112.9 | 50.0 | −276.6 | 25.0 | 1330.0 | 30.5 | −22.6 | 942.1 | 3.2 |
| $RBa_2Cu_3O_6$ (tetragonal) | | | | | | | | | |
| Gd ME [11] | 113.9 | | | | ($V_{zz} = -5.3 \times 10^{21}$ V m$^{-2}$, $\eta = 0.03 \approx 0$) | | | | |
| Ho INS [15] | 167.0 | | −230.1 | | 1041.5 | 25.6 | | 835.4 | |
| Ho INS [5] | 56.5 | | −272.6 | | 1356.6 | 29.7 | | 942.1 | |
| Tm theory [16] | 70.4 | | −252.6 | | 1334.5 | 31.8 | | 806.8 | |
| $RBa_2Cu_4O_8$ | | | | | | | | | |
| Gd ME [17] | 136.3 | 50.4 | | | ($V_{zz} = -6.34 \times 10^{21}$ V m$^{-2}$, $\eta = 0.37$) | | | | |
| Ho INS [6] | 174.2 | 43.6 | −220.4 | −4.8 | 1041.5 | 26.8 | −24.9 | 835.4 | −4.4 |
| Ho INS [7] | 199.6 | 50.8 | −220.4 | 0.0 | 1065.7 | 26.9 | −24.9 | 841.7 | −6.2 |
| Tm $\chi$ [8] | 63.88 | 31.94 | −182.8 | 12.35 | 839.9 | 21.58 | −12.80 | 648.0 | −9.06 |
| Tm INS [9] | 51.90 | −79.85 | −227.3 | 49.41 | 1408.1 | 21.58 | 2.88 | 805.7 | −100.7 |
| Tm NMR [4] | 65 | 72 | −230 | 32 | 1325 | 29 | 44 | 804 | −2 |

An extensive range of measurement techniques has been applied to this problem: inelastic neutron scattering (INS), nuclear magnetic resonance (NMR), DC susceptibility ($\chi$), specific heat, Mössbauer effect (ME) and optical spectroscopy. Ishigaki *et al* [4] recently provided a summary of experimentally determined CF parameters for both 1–2–3-type and 1–2–4-type superconductors and an updated version of this summary is included

in table 1. To facilitate comparison with the earlier summary of Ishigaki *et al*, the $A_n^m$ employed in this work have been defined in the same way and the same units of $cm^{-1}$ have been employed. Generally speaking, the higher-rank CF parameters behave as expected, and the rank-2 parameters do vary from compound to compound. However, there is also considerable variation for rank-2 parameters derived using different techniques, and for rank-2 parameters derived by different research groups using the same technique. To some extent this may be attributed to the need to fit a relatively large number of parameters to the experimental data. If we focus on the Ho INS results of Staub *et al* [5], both rank-2 parameters are found to diminish with oxygen depletion of the 1–2–3-type compounds. According to the Ho INS results of Furrer [6] and Roessli *et al* [7], the rank-2 parameters for the 1–2–4 compound are somewhat larger than those for $HoBa_2Cu_3O_7$. However, according to the magnetic susceptibility results of Nichols *et al* [8], the INS results of Santini *et al* [9] and the NMR results of Ishigaki *et al* [4], the $A_2^0$-parameter for $TmBa_2Cu_4O_8$ is closer to that determined by Staub *et al* for $HoBa_2Cu_3O_6$ [5].

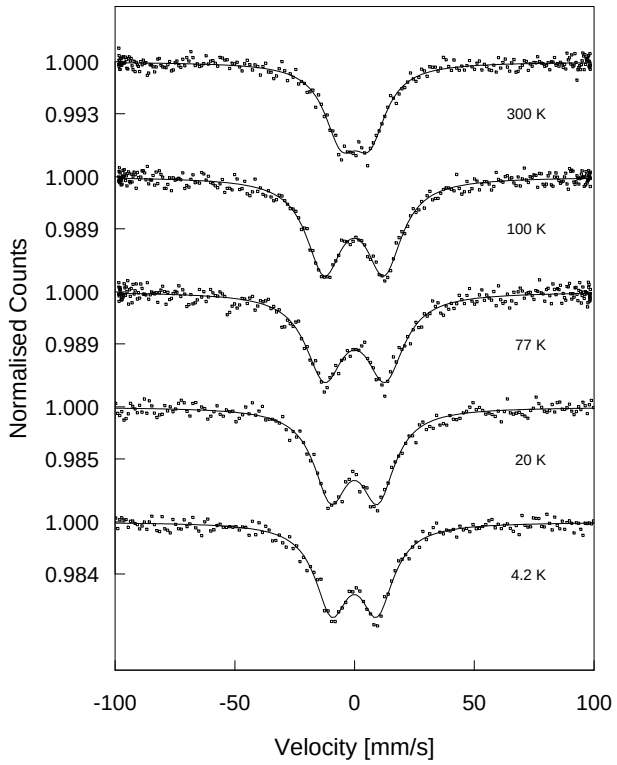


**Figure 1.** Representative $^{169}$Tm Mössbauer spectra for $TmBa_2Cu_4O_8$.

Until now, inelastic neutron scattering with R = Ho has been the only technique that has provided CF data for the full range of 1–2–3 and 1–2–4 compounds. This paper provides new $^{169}$Tm Mössbauer results for Tm 1–2–4 and an oxygen-depleted Tm 1–2–3 compounds which combine with earlier results to form a similarly complete set of $^{169}$Tm Mössbauer measurements. The approach adopted will be to test the various sets of CF parameters already published for Tm 1–2–4 against these new data and then, commencing with the existing Ho INS parameters, to obtain CF fits for the full set of $^{169}$Tm results.

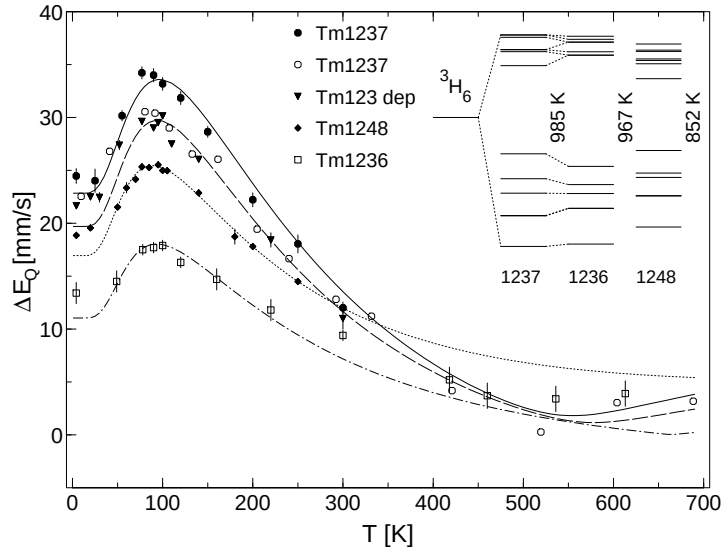


**Figure 2.** The temperature dependence of the electric quadrupole splitting, $\Delta E_Q$, determined from $^{169}$Tm Mössbauer spectra for $TmBa_2Cu_3O_7$ (○ [21], ● [13]), oxygen-depleted $TmBa_2Cu_3O_{6.64}$ (▼, this work), $TmBa_2Cu_3O_6$ (□ [13]) and $TmBa_2Cu_4O_8$ (♦, this work). The fitted curves and associated crystal-field-level schemes for each system are discussed in the text.

## 2. Experimental details and results

The $TmBa_2Cu_4O_8$ sample was made by pelletizing stoichiometric quantities of $Tm_2O_3$, $Ba(NO_3)_2$ and fine-particle CuO, and heating to about 700 °C to ensure decomposition of the $Ba(NO_3)_2$. The specimen was then subjected to repeated cycles of grinding, pelletizing and reaction at 900–940 °C under oxygen pressures greater than 10 atm, with a final sinter at 960 °C and 60 atm oxygen pressure. The sample was characterized by x-ray powder diffraction and by electrical resistivity measurements which yielded a superconducting transition temperature of $T_c = 80$ K.

The source used for the $^{169}$Tm Mössbauer spectroscopy was a 20 mg, 13 mm diameter, $^{168}Er_{0.15}Al_{0.85}$ foil activated by neutron irradiation. Absorbers were made by mixing approximately 9 mg cm$^{-2}$ of $TmBa_2Cu_4O_8$ powder with $CB_4$ as a filler. The absorbers were cooled in a transmission geometry cryostat, the source being mounted externally on a transducer with sinusoidal motion. The spectra were calibrated against a standard $TmF_3$ absorber at 4.2 K. Spectra were taken over the temperature range of 4.2–300 K.

Representative $^{169}$Tm Mössbauer spectra for the $TmBa_2Cu_4O_8$ sample, together with fits, are shown in figure 1. The spectra were fitted with a single quadrupole-split doublet, giving the quadrupole splitting, $\Delta E_Q$, for each spectrum. As anticipated, there is no indication of magnetic order down to 4.2 K. Other members of this isostructural series are observed to order at temperatures typically less than 2 K [7, 17–19]. The temperature variation of the quadrupole splitting, $\Delta E_Q$, is shown in figure 2 where it is compared with similar results for $TmBa_2Cu_3O_7$ and $TmBa_2Cu_3O_6$. Also included are the results obtained in this work for an oxygen-depleted $TmBa_2Cu_3O_{7-\delta}$ sample prepared by reaction in air at ambient pressure. The value of $\delta = 0.34(1)$ was arrived at by comparison of the specimen's measured lattice parameters with those published in the literature for specimens of known oxygen depletion;

the cell volume was within experimental error of that for a specimen reported on by Tarascon *et al* [20].

The temperature dependence of the quadrupole splitting, $\Delta E_Q$, is a consequence of the CF interaction acting at the thulium sites (as described in more detail in section 3). Its form is therefore a *fingerprint* which can be used for an initial qualitative comparison of local electrostatic environments in different materials. It normally varies considerably from specimen to specimen. However, from figure 2 it is seen to be of similar form for all of the systems considered here. That is, in each case $\Delta E_Q$ exhibits a broad maximum at about 100 K. This common feature is associated with the dominant short-range, higher-rank CF terms that vary only marginally. The fact that the broad peak is centred on the temperature region in which the superconducting transition occurs is coincidental and does not imply that there is an interconnection. In support of this, it should be noted that $TmBa_2Cu_3O_6$ is not a high-temperature superconductor. From figure 2, the maximum value of $\Delta E_Q$ is observed to decrease with increasing oxygen depletion of the 1–2–3 system. This is associated with the corresponding diminishment of the long-range, rank-2 CF parameters as referred to in the introduction. Note that the curve for the nominally $TmBa_2Cu_3O_7$ specimen of Gubbens *et al* [21] coincides with the curve for $TmBa_2Cu_3O_{6.64}$ measured in this work. Given that these curves are clearly separated from the curve for the $TmBa_2Cu_3O_7$ specimen of Bergold *et al* [13], the specimen employed by Gubbens *et al* was most probably depleted. The maximum value for the $TmBa_2Cu_4O_8$ curve lies approximately midway between the maximum values for $TmBa_2Cu_3O_7$ and $TmBa_2Cu_3O_6$, which suggests that the rank-2 parameters should also lie between the parameter values for these two compounds. This is more in keeping with the conclusions of Ishigaki *et al* [4] than with the Ho INS results of Furrer [6] and Roessli *et al* [7]. However, the high-temperature tail of the $TmBa_2Cu_4O_8$ curve appears to flatten out earlier than those for the curves of the 1–2–3-type compounds. Since the high-temperature $\Delta E_Q$ is influenced most by the rank-2 CF parameters, there would appear to be more than just a simple scaling effect involved.

## 3. Crystal-field analysis

The quadrupole splitting, $\Delta E_Q$, determined from a $^{169}$Tm Mössbauer spectrum is a measure of the strength of the electric quadrupole interaction and is given by

$$\Delta E_Q = \frac{1}{2} e Q V_{zz} \left(1 + \frac{\eta^2}{3}\right)^{1/2} \tag{4}$$

where $\eta = (V_{xx} - V_{yy})/(V_{zz})$ is the asymmetry parameter, $V_{xx}$, $V_{yy}$ and $V_{zz}$ are the principal components of the electric field gradient (efg), and $Q$ is the nuclear quadrupole moment of the 8.4 keV, $I = 3/2$ nuclear level. The CF influences the efg in two ways. First it distorts the 4f shell of the trivalent rare-earth ion resulting in a temperature-dependent efg which depends on the full CF Hamiltonian. Secondly, apart from different shielding effects, the lattice efg can act directly on the nucleus to give a constant contribution which depends only on the rank-2 CF parameters. For the situation where the charge distribution responsible for the CF does not overlap with the 4f shell, the expressions for the two efg contributions are relatively straightforward [22, 23]. For tetragonal site symmetry, $\eta = 0$ and the total $V_{zz}$-component is given by

$$V_{zz} = -\frac{\theta_2 e}{4\pi\epsilon_0} \langle r^{-3} \rangle_{4f} (1 - R_Q) F_2^0 \langle O_2^0(J) \rangle_T - \frac{4(1 - \gamma_\infty)}{e(1 - \sigma_2)\langle r^2 \rangle_{4f}} L_2^0 A_2^0 \tag{5}$$

where $\langle O_2^0(J)\rangle$ is a Boltzmann average of the Stevens operator over the thermally populated CF levels, $F_2^0 = L_2^0 = 1$, and all of the other symbols take their usual meanings. For the case of orthorhombic site symmetry, $\eta \neq 0$ and an expression similar to (5) relates $V_{xx} - V_{yy}$ to $\langle O_2^2\rangle_T$ and $A_2^2$ with $F_2^2 = 3$ and $L_2^2 = 1$. Because $Gd^{3+}$ is an *S*-state ion, there is no 4f contribution to the efg acting at its nucleus. Hence $^{155}$Gd Mössbauer spectroscopy plays an important role in estimating the constant lattice efg contribution for a series of isostructural rare-earth compounds. Alternatively, via the second part of (5), the measured lattice efg contribution can be used to provide estimates of rank-2 CF parameters for isostructural compounds with rare-earth ions which are not *S*-state. For this purpose, values of $(1 - \gamma_\infty)_{Gd^{3+}} \simeq 60$ [24] and $Q(^{155}\text{Gd}) = 1.3$ b [25] are assumed here.

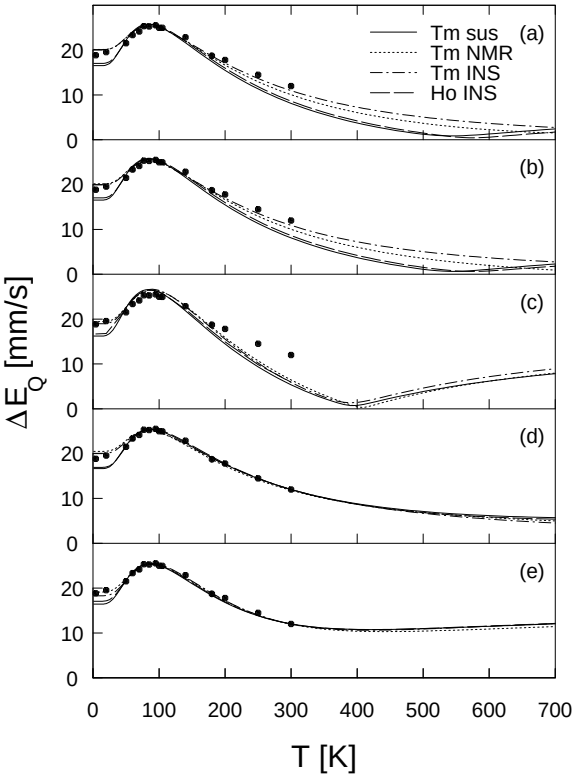


**Figure 3.** The temperature dependence of $\Delta E_Q$ for $TmBa_2Cu_4O_8$ with theory curves fitted by varying only the rank-2 crystal-field parameters $A_2^0$ and $A_2^2$ as described in the text.

In what follows, the three sets of CF parameters published for $TmBa_2Cu_4O_8$ [8, 9, 4] plus the most recent set of INS-determined parameters for $HoBa_2Cu_4O_8$ (i.e. the last four rows of table 1) are adopted as starting parameters for theoretical fits to the present $^{169}$Tm $\Delta E_Q$ data for $TmBa_2Cu_4O_8$. At first glance, the Tm INS CF parameter set seems to be exceptional in that it provides a negative $A_2^2$-value. However, the positive sign of $A_2^2$ can be restored by a coordinate frame rotation through 90° about the *c*-axis. Although this would simultaneously reverse the signs of $A_4^2$, $A_6^2$ and $A_6^6$, these parameters are associated with the slight orthorhombic site distortion and are usually determined with large experimental uncertainties [5, 7]. Theoretical calculations with these parameters reversed in sign verified that they were of little consequence for $\Delta E_Q$ at the $^{169}$Tm nucleus. In the case of the Ho

INS CF parameters, they were converted for R = Tm via the ideal relationship

$$A_n^m(\mathrm{Tm}^{3+}) = A_n^m(\mathrm{Ho}^{3+})\frac{[(1-\sigma_n)\langle r^n\rangle_{4\mathrm{f}}]_{\mathrm{Tm}^{3+}}}{[(1-\sigma_n)\langle r^n\rangle_{4\mathrm{f}}]_{\mathrm{Ho}^{3+}}}. \tag{6}$$

For each of these four sets, the higher-rank CF parameters were fixed at their respective literature values and only the rank-2 CF parameters were varied to obtain best fits to the experimental $\Delta E_Q$ data using five different approaches.

(a) $A_2^0$ varied with the ratio $A_2^2/A_2^0$ fixed at the literature value.
(b) $A_2^0$ varied with the ratio $A_2^2/A_2^0$ fixed to that determined by $^{155}$Gd Mössbauer spectroscopy for $GdBa_2Cu_4O_8$ [17].
(c) $A_2^0$ varied with the ratio $A_2^2/A_2^0$ fixed at the literature value; lattice efg contributions set independently at values determined for $GdBa_2Cu_4O_8$ by $^{155}$Gd Mössbauer spectroscopy.
(d) $A_2^0$ and $A_2^2$ varied.
(e) $A_2^0$ and $A_2^2$ varied; lattice efg contributions set independently at values determined for $GdBa_2Cu_4O_8$ by $^{155}$Gd Mössbauer spectroscopy.

The theoretical $\Delta E_Q$ calculations employed shielding parameters based on the recommended value of $\rho_1 = Q(1-R_Q)\langle r^{-3}\rangle_{4\mathrm{f}} = -15.2$ b au$^{-3}$ and the theoretical value of $\rho_2 = Q(1-\gamma_\infty)/[(1-\sigma_2)\langle r^2\rangle_{4\mathrm{f}}] = -381$ b au$^{-2}$ [26]. The theoretical curves are shown in figure 3 (labelled (a) to (e) according to the above approaches) and the fitted rank-2 parameters are presented in table 2 where they are compared with the original literature values. Overall, the closest fits with the most reasonable rank-2 parameters are achieved with approach (d) for the higher-rank parameters from Tm susceptibility, Tm NMR and Ho INS. These fits require the $A_2^2$-value to be larger than $A_2^0$ which is contrary to the original Ho INS result.

**Table 2.** Rank-2 crystal-field parameters (cm$^{-1}$) obtained from the fits to the temperature dependence of the quadrupole splitting, $\Delta E_Q$, of $TmBa_2Cu_4O_8$. Each set of fits corresponds to the equivalent set of curves shown in figure 3. The Ho-based crystal-field parameters were converted to values appropriate to Tm using (6).

| | Susceptibility | | NMR | | Tm INS | | Ho INS | |
|---|---|---|---|---|---|---|---|---|
| | $A_2^0$ | $A_2^2$ | $A_2^0$ | $A_2^2$ | $A_2^0$ | $A_2^2$ | $A_2^0$ | $A_2^2$ |
| Literature | 63.9 | 31.9 | 65.0 | 72.0 | 51.9 | 79.8 | 197.7 | 50.3 |
| (a) | 74.0 | 37.0 | 31.3 | 34.7 | 1.3 | 2.0 | 67.5 | 17.2 |
| (b) | 73.9 | 27.3 | 31.4 | 25.5 | 0.8 | 0.3 | 67.5 | 25.0 |
| (c) | 96.6 | 48.3 | 73.8 | 81.7 | 51.1 | 78.8 | 92.7 | 23.6 |
| (d) | 65.2 | 142.2 | 22.7 | 145.8 | −3.8 | 90.0 | 60.2 | 138.3 |
| (e) | 82.6 | 121.7 | 55.4 | 298.8 | 32.2 | 283.2 | 78.9 | 126.6 |

Given the availability of CF parameter sets derived using Ho INS for the full 1–2–3-type compound series, and given the previous success of Bergold *et al* [13] with their $TmBa_2Cu_3O_7$ results, it was decided to fit all $^{169}$Tm Mössbauer data for the 1–2–3-type compounds using approach (d) and starting with converted Ho INS parameters. The theory curves generated in this way are shown in figure 2, together with their corresponding CF schemes for the $^3H_6$ ground state of the $Tm^{3+}$ ion. The fitted rank-2 parameters are summarized in table 3.

The theory curves closely reflect the overall form of the experimental data. However, the fitted $\Delta E_Q$ values are slightly undervalued in the lower-temperature region of $T \leqslant 50$ K as

**Table 3.** A summary of rank-2 crystal-field parameters obtained from theory fits to experimental $\Delta E_Q(^{169}\mathrm{Tm})$ data using approach (d) and starting with converted Ho INS parameters, which are included in parentheses. Refer to the text for details.

| | $TmBa_2Cu_3O_{7-\delta}$ | | | |
|---|---|---|---|---|
| | $\delta = 0$ | $\delta = 0.34$ | $\delta = 1$ | $TmBa2Cu_4O_8$ |
| $A_2^0$ ($cm^{-1}$) | 128.9 (141.0) | 95.4 (111.8) | 39.3 (55.9) | 60.2 (197.6) |
| $A_2^2$ ($cm^{-1}$) | 87.7 (95.8) | 42.2 (49.5) | 0.0 (0.0) | 138.3 (50.3) |
| $^{169}$Tm data | [13] | This work | [13] | This work |
| Ho INS data | [5] | [5] | [5] | [7] |

well as in the high-temperature tail for $TmBa_2Cu_3O_6$. The latter is probably a consequence of the larger uncertainty in the $TmBa_2Cu_3O_6$ data due to the poorer resolution of the quadrupole-split doublet spectrum. For the 1–2–3-type compounds, the starting values of both $A_2^0$ and $A_2^2$ converted from Ho INS needed to be reduced by approximately the same amount (consistent with approach (a), and consistent with the earlier analysis of $TmBa_2Cu_3O_7$ [13]), and this amount increased with oxygen depletion. This is quite different to the fit for $TmBa_2Cu_4O_8$ which required the converted Ho INS starting value of $A_2^0$ to be decreased but the value of $A_2^2$ to be increased.

## 4. Discussion

The disparity between the $^{169}$Tm data and the Ho INS CF parameters observed in this work suggests that the rank-2 component of the CF differs across the heavy rare-earth series, that this difference becomes more significant with increased oxygen depletion of the 1–2–3-type compounds, and that it is most significant for the 1–2–4-type compounds. In this regard, the CF parameters derived for $TmBa_2Cu_4O_8$ using Tm INS [9] also differ from those converted from Ho INS and imply a reduced $A_2^0$ with $A_2^2$ slightly larger than $A_2^0$, which is in the direction of the fit to the $^{169}$Tm data. However, CF parameters for isostructural compounds of different heavy rare earths are usually more consistent and Ho and Tm are next-nearest neighbours in the lanthanide series. Experience tells us that CF parameter conversions should be more reliable in these circumstances.

An alternative explanation might be sought in the nature of the INS and $^{169}$Tm Mössbauer techniques themselves. INS is a direct spectroscopic method which determines the CF levels at a single temperature. Nonetheless, the variation in CF parameters using this technique (table 1) suggest that the interpretation of such data is not trivial. By comparison, $^{169}$Tm Mössbauer spectroscopy provides the temperature dependence of the quadrupole splitting, $\Delta E_Q$, over a wide temperature range, which is then analysed in terms of a single set of CF parameters. It is possible, therefore, that the discrepancy may be associated with a CF parameter variation arising out of a temperature dependence of the lattice parameters. However, literature lattice parameters show only a small change (less than 1% over 4.2 K to 300 K) with temperature and, for example, this change is no larger for oxygen-depleted $YBa_2Cu_3O_{7-\delta}$ and $YBa_2Cu_4O_8$ than for $YBa_2Cu_3O_7$ [27–29].

Another possible explanation is associated with the dual role of the CF interaction with respect to the efg induced at the $^{169}$Tm nucleus. Overlap of the lattice charge distribution

and the 4f shell can result in different effective CF parameters being required for the CF splitting of the 4f shell and for the direct lattice efg contribution, as was first demonstrated theoretically by Coehoorn for rare-earth intermetallics [30]. This was the rationale behind fit approaches (c) and (e). However, these approaches did not offer significantly improved theory fits. Finally, the operator-equivalent formalism of (1) assumes that higher electronic multiplets can be ignored. For guidance, it is useful to compare the more recent Ho INS work of Staub *et al* [5], which employed intermediate coupling and $J$-mixing, with the earlier Ho INS work of Furrer *et al* [12] and Allenspach *et al* [15], which assumed a single multiplet. However, this suggests that the single-multiplet $^{169}$Tm analysis would lead to CF parameters which were too large rather than too small. Furthermore, the calculations reported here using as-converted Ho INS parameters indicate that the overall CF splitting of the $Tm^{3+}$ ground term decreases marginally with depletion and is smallest for 1–2–4, implying reduced multiplet overlap. On the basis of these considerations, we are led to conclude that the discrepancies between rank-2 CF parameters determined for $HoBa_2Cu_4O_8$ and $TmBa_2Cu_4O_8$ are genuine.

## 5. Conclusions

New Mössbauer spectroscopy measurements of the temperature-dependent $^{169}$Tm quadrupole splitting for $TmBa_2Cu_4O_8$ and an oxygen-depleted $TmBa_2Cu_3O_{6.64}$ specimen complement earlier measurements for $TmBa_2Cu_3O_7$ and $TmBa_2Cu_3O_6$. The collected data curves reveal a smooth decrease in maximum $\Delta E_Q$ with oxygen depletion of the 1–2–3-type compounds, with the $TmBa_2Cu_4O_8$ value located approximately midway between the $TmBa_2Cu_3O_7$ and $TmBa_2Cu_3O_6$ extremes. These observations support the conclusions of Ishigaki *et al* [4]. A systematic comparison with CF parameters derived from Ho INS investigations indicates a disparity between the rank-2 CF parameters of Tm- and Ho-based compounds. This disparity increases with oxygen depletion of the 1–2–3 compounds and is maximum for the 1–2–4-type compound.

## Acknowledgments

This work was supported by a grant for source irradiation from the Australian Institute of Nuclear Science and Engineering. SJH acknowledges University College and School of Physics support for the final stages of his PhD candidature.

## References

[1] Dunlap B D, Slaski M, Hinks D G, Soderholm L, Beno M, Zhang K, Segre C, Crabtree G W, Kwok W K, Malik S K, Schuller I K, Jorgensen J D and Sungaila Z 1987 *J. Magn. Magn. Mater.* **68** L139–44

[2] Mori K, Kawaguchi Y, Ishigaki T, Katano S, Funahashi S and Hamaguchi Y 1994 *Physica* C **219** 176–82

[3] Jorgensen J D, Beno M A, Hinks D G, Soderholm L, Volin K J, Hitterman R L, Grace J D, Schuller I K, Segre C U, Zhang K and Kleefisch M S 1987 *Phys. Rev.* B **36** 3608–16

[4] Ishigaki T, Mori K, Bakharev O N, Dooglav A V, Krjukov E V, Lavizina O V, Marvin O B, Mukhamedshin I R and Teplov M A 1995 *Solid State Commun.* **96** 465–9

[5] Staub U, Mesot J, Guillame M, Allenspach P, Furrer A, Mutka H, Bowden Z and Taylor A 1994 *Phys. Rev.* B **50** 4068–74

[6] Furrer A 1993 *Selected Topics in Superconductivity (Frontiers in Solid State Sciences 1)* ed L C Gupta and M S Multani (Singapore: World Scientific) pp 349–70

[7] Roessli B, Fischer P, Guillame M, Mesot J, Staub U, Zolliker M, Furrer A, Kaldis E, Karpinski J and Jilek E 1994 *J. Phys.: Condens. Matter* **6** 4147–52

[8] Nichols D H, Dabrowski B, Welp U and Crow J E 1994 *Phys. Rev.* B **49** 9150–6
[9] Santini P, Amoretti G and Caciuffo R 1994 *Physica* B **193** 221–31
[10] Bornemann H J, Czjzek G, Ewert D, Meyer C and Renker B 1987 *J. Phys. F: Met. Phys.* **17** L337–43
[11] Wortmann G, Kolodziejczyk A, Simmons C T and Kaindl G 1988 *Physica* C **153–155** 1547–8
[12] Furrer A, Brüesch P and Unternährer P 1988 *Phys. Rev.* B **38** 4616–23
[13] Bergold M, Wortmann G and Stewart G A 1990 *Hyperfine Interact.* **55** 1205–12
[14] Goodman G L, Loong C K and Soderholm L 1991 *J. Phys.: Condens. Matter* **3** 49–67
[15] Allenspach P, Furrer A, Brüesch P, Marsolais R and Unternährer P 1989 *Physica* C **157** 58–64
[16] Lavizina O V 1995 *Phys. Solid State* **37** 1228–30
[17] Bornemann H J, Morris D E, Steinleitner C and Czjzek 1991 *Phys. Rev.* B **44** 12 567–70
[18] Zhang H, Lynn J W, Li W H and Clinton T W 1990 *Phys. Rev.* B **41** 11 229–36
[19] Roessli B, Fischer P, Zolliker M, Allenspach P, Mesot J, Staub U, Furrer A, Kaldis E, Bucher B, Karpinski J, Jilek E and Mutka H 1993 *Z. Phys.* B **91** 149–53
[20] Tarascon J M, McKinnon W R, Greene L H, Hull G W and Vogel E M 1987 *Phys. Rev.* B **36** 226–34
[21] Gubbens P C M, van Loef J J, van der Kraan A M and de Leeuw D M 1988 *J. Magn. Magn. Mater.* **76–77** 615–6
[22] Barnes R G, Mössbauer R L, Kankeleit E and Poindexter J M 1964 *Phys. Rev.* A **136** 175–89
[23] Stewart G A 1985 *Hyperfine Interact.* **23** 1–16
[24] Gupta R P and Sen S K 1973 *Phys. Rev.* A **7** 850–8
[25] Tanaka Y, Laubacher D B, Steffen R M, Shera E B, Wohlfahrt H D and Hoehn M V 1982 *Phys. Lett.* **108B** 8–10
[26] Stewart G A, Day R K, Dunlop J B and Price D C 1988 *Hyperfine Interact.* **40** 339–42
[27] Johnston D C, Jacobson A J, Newsam J M, Lewandowski J T, Goshorn D P, Xie D and Yelon W B 1987 *Chemistry of the High-Temperature Superconductors (ACS Symposium Series 351)* ed D L Nelson, M S Whittingham and F G Thomas (Washington, DC: American Chemical Society) ch 14, pp 136–51
[28] Cava R J, Krajewski J J, Peck W F, Batlogg B, Rupp L W Jr, Fleming R M, James A C W P and Marsh P 1989 *Nature* **338** 328–30
[29] Kaldis E, Fischer P, Hewat A W, Karpinski J and Rusiecki S 1989 *Physica* C **159** 668–80
[30] Coehoorn R 1991 *Supermagnets, Hard Magnetic Materials (NATO ASI Series C, vol 331)* ed G J Long and F Grandjean (Dordrecht: Kluwer) ch 8, pp 133–70